An Optical Signal Correlated with the Allosteric Transition in *Scapharca inaequivalvis* HbI†

Jeffry C. Nichols,*,‡,§ William E. Royer, Jr.,§ and Quentin H. Gibson§

Department of Biochemistry and Molecular Pharmacology, University of Massachusetts Medical School, Worcester, Massachusetts 01655, and Chemistry Department, Worcester State College, Worcester, Massachusetts 01602

Received July 18, 2006; Revised Manuscript Received October 12, 2006

ABSTRACT: The transient absorbance change within the first 2 μs of photolysis of COHbI (from *Scapharca inaequivalvis*) reported by Chiancone et al. [Chiancone, E., Elber, R., Royer, W. E., Regan, R., and Gibson, Q. H. (1993) *J. Biol. Chem. 268*, 5711−5718] has been studied in several mutants. Evidence is presented that this change (*rts*) is associated with the allosteric transition between R and T states. Two different *rts* spectra relate to Hb_2 and Hb_2CO. No *rts* has been observed for mutants at position 97 (normally Phe). Correlation of ligand binding and *rts* shows that protein function changes at or near the rates of *rts*, typically, 2×10^6 s^{-1} (Hb_2) and 5×10^5 s^{-1} (Hb_2CO). Unique values of allosteric parameters for several mutants have been obtained by combining kinetic and equilibrium data. The effect of mutation on function thus may be assigned to allostery or to a change in intrinsic heme reactivity.

Cooperativity in ligand binding by mammalian hemoglobins, expressed in their sigmoid equilibrium curves, was established approximately a century ago. These studies initiated attempts, still ongoing, to describe the curves in physicochemical terms. Difficulties in studying these hemoglobins have arisen from (a) two kinds of subunits, (b) four subunits per molecule, (c) a strong dependence on pH and salts, and (d) tetramer to dimer dissociation. Clearly, a dimeric hemoglobin would be much easier to study. There are, however, few dimeric types of hemoglobin and fewer still that bind ligands cooperatively. The hemoglobin from *Scapharca inaequivalvis* that has two identical subunits, no effect of pH and salts, marked cooperativity, and a very small dimer to monomer dissociation constant even when liganded perhaps comes closest to the ideal.

This homodimeric hemoglobin was first studied in relation to an Adriatic clam fishery. References to the early work may be found in the work of Antonini et al. (*2*). In that paper, the kinetics of the reactions of the native protein with oxygen and carbon monoxide were described in terms of the two-state model (MWC)[1] of Monod, Wyman, and Changeux (*3*). They noted, however, that unique values of the allosteric parameters could not be assigned from ligand binding studies alone because of the close correlation between *L* (the ratio of the R and T forms of deoxyhemoglobin) and *c* (the change in *L* on binding each ligand molecule). The structures of both liganded and deoxy forms of the wild type and of many mutants have been determined at high resolution (*4*, *5*). Unlike mammalian hemoglobins, there are no major quaternary structural changes on ligand binding, allowing fully cooperative binding of oxygen to crystals (*6*). However, residue F97 does move away from the heme group, and water molecules in the interface between the subunits change in number and position. The importance of residue 97 has been underscored by site-directed mutagenesis (*7*, *8*) and the role of interfacial water probed by the T72V isosteric substitution (*9*, *10*). It does not alter the structure apart from these water molecules, but the mutation increases the oxygen affinity some 50-fold. Royer et al. (*9*) have shown that the kinetic and equilibrium effects may be explained by changing the MWC parameter *L* without any alteration of *c*. We now describe a spectrophotometric signal (*rts*), present evidence of its relation to allostery, and illustrate how the properties of F97 mutants (*8*) may be used to assign unique values to allosteric parameters *L* and *c* in the MWC model. Edelstein (*11*) proposed that the rough relation between affinity and cooperativity (expressed as Hill's *n*, a measure of inflection of a sigmoid curve) of several naturally occurring mutants of human hemoglobin may be explained in terms of the MWC model on the assumption that the mutants share common tense and relaxed (T and R, respectively) states. An analogous relation has been found among mutants of *Scapharca*, and both the principle and deviations from it contribute to the understanding of the detailed mechanism.

MATERIALS AND METHODS

Flash photolysis data were collected by feeding the output of a fast photomultiplier into the 50 Ω input of a Tektronix model TDS620 oscilloscope. During data collection, a 75 W xenon arc light source was pulsed using a lumped component network to flatten the peak of the output pulse. No corrections were required for total collection times of

† This work was supported by the National Institutes of Health (Grants DK43323 and GM66756 to W.E.R.).

* To whom correspondence should be addressed. Phone: (508) 929-8465. Fax: (508) 929-8171. E-mail: Jeffry.Nichols@worcester.edu.

‡ University of Massachusetts Medical School.

§ Worcester State College.

[1] Abbreviations: Hb, hemoglobin; HbI, *Scapharca* dimeric hemoglobin I; *rts*, spectrophotometric signal correlated with the allosteric change from the T to R state; p_{50}, partial pressure of oxygen at which 50% of ligand binding sites are occupied; rms, root-mean-square; MWC model, Monod, Wyman, and Changeux two-state model; *L*, ratio of R to T forms of deoxy Hb; *c*, change in *L* on binding each ligand molecule.

10.1021/bi061451k CCC: $33.50
Published on Web 12/19/2006

up to 10 μs. An interval of 6 s between laser flashes was obtained by counting the pump flashes of the laser both to minimize heating of the sample and to standardize the charging time for the pulser network. The data were displayed as collected, and collection continued until a satisfactory signal was obtained, using up to 50 flashes. Data were collected between 450 and 400 nm at intervals of 5 nm. In most cases, neutral density filters were used to give five or six levels of photolysis. The 8 bit resolution of the oscilloscope is not sufficient to display the relatively small R−T signal, so a second expanded trace was also collected on a more sensitive scale. The expanded traces by themselves do not provide meaningful absorbance information because the trace is off screen until the laser fires. The change in absorbance from zero time to the end of the normal trace served to scale the expanded trace. The scaled traces were represented as the sum of two, or more rarely, three exponentials. The data at all wavelengths and a single light level were fitted as a group, using the same rates for the components. The correlations from the covariance matrix were used as an index of the interdependence of the rate constants. This procedure separated the contributions of geminate recombination and the *rts* signal. In addition to the difference in spectrum, geminate recombination was usually 1 order of magnitude faster than the *rts* signal. In analysis, the expanded traces were usually treated as starting from time zero. When treated as differences from the last recorded data, slower processes would be ignored, but in practice, comparisons between the two methods seldom yielded discrepancies, suggesting the absence of slower processes apart from bimolecular recombination. This rate was not taken into account, as it was always more than 2 orders of magnitude slower than the first-order processes. Comparisons of the effect of the change in the level of photolysis on the amplitude of the *rts* signal used the absorbance at the end of the normal traces, when geminate and R−T processes were complete, as a measure of effective photolysis, and the *rts* signal was taken as the sum of the weighting coefficients for the appropriate rate component between 420 and 435 nm.

RESULTS AND DISCUSSION

Nature and Assignment of Signal. An extract from the *rts* data collected during the first 1.6 μs after photolysis of wild-type COHbI is shown in Figure 1. A single shot at one wavelength shows ligand binding and the *rts* signal and gives an idea of their relative amplitudes and time scales (Figure 1A). Eleven wavelengths were used with six light levels at each wavelength and 400 points in each trace; an extract is shown in Figure 1B. In analysis, the data were first described by fitting the full photolysis data set with two exponentials. There were two rates at each light level, an invariant one of 2.2×10^7 s^{-1} and another dropping from 2.0×10^6 to $\sim 5.0 \times 10^5$ s^{-1} as the photolysis level decreased. The precision at low light is much lower because of increased noise. The rates are only weakly correlated, with a value from the covariance matrix of 0.13. At each wavelength and level of photolysis, the coefficients of the exponentials define the contributions of the underlying processes at that point and are plotted to give the spectrum of each component (Figure 1C). The spectrum and rate of the faster component (top curve) suggest its source is geminate recombination. The spectrum is that of ligand binding, and the rate of 2.2×10^7 s^{-1} is the same as that for oxygen. Both components scale with the level of hemoglobin photolysis. The geminate rebinding component corresponds to 4.2% of the total ligand binding difference spectrum (Figure 1D).

As the products of photolysis are Hb_2 and Hb_2CO, it is plausible to associate their formation with the second rate. Immediately after photolysis, the distribution between R and T states of both products is that of $Hb_2(CO)_2$. Royer et al. (*9*) have suggested that ~80% of wild-type $Hb_2(CO)_2$ is in the R state and that both Hb_2CO and Hb_2 are more than 97% T state at equilibrium. It follows that both photoproducts (Hb_2 and Hb_2CO) may be expected to relax to the T state. As the level of photolysis falls, the proportion of Hb_2CO relative to Hb_2 increases and its R to T rate has a growing influence on the overall observed *rts* rate. The data were therefore refit using three exponentials giving the rates of three processes as 1.37×10^7, 2.1×10^6, and 0.9×10^5 s^{-1} for the full data set and all six light levels. The rms residual remained at 0.001: the largest correlation of 0.38 was between the two *rts* rates. Neither *rts* rate was strongly correlated with the geminate rate (0.23 and 0.25). The use of three exponentials therefore appears to be justified, although the difference between the two *rts* rates was too small to be apparent when data for single light levels were examined separately. The three spectra are presented in Figure 2A. Comparison shows that the *rts* signal in Figure 1C is indeed the sum of the two *rts* spectra in Figure 2A. Analogous results obtained with L73M, F97Y, and T72V are also presented in Figure 2; they will be discussed later.

Further evidence of a relation between the *rts* signal and conformation change comes from the high-affinity species F97L, F97Y, and F97V, none of which has an *rts* signal. F97Y, in particular, has been studied in detail recently (*8*). The characteristic movement of residue F97, packing close to the heme in the deoxy form and moving out on ligand binding, does not occur. Several features of the behavior of this mutant following photolysis are presented in Figures 2C and 3. There are two rapid geminate reactions with different difference spectra and rates, and as already reported (*8*), bimolecular binding of CO is also biphasic. Although the static spectra of oxy and carboxy F97Y hemoglobins are closely similar to those of the wild type, the spectrum of deoxy F97Y has a lower absorbance at the Soret maximum (Figure 3). There is apparently more than one stable conformation. The longer-wavelength species has a geminate rate of 7.4×10^7 s^{-1} and accounts for some 40% of the total geminate reaction. The rate for the slower component is 1.0×10^7 s^{-1}. The F97V mutant behaves similarly (not illustrated). The high-affinity mutants F97L, F97Y, and F97V also share a large observed rate of oxygen binding of 40−50 μM^{-1} s^{-1} (cf. the wild-type rate of 17 μM^{-1} s^{-1}) and have the same rate of oxygen dissociation (2.8 s^{-1}) measured either with dithionite or by replacement of oxygen with CO. This commonality leads us to suggest that these rates may define a standard R state.

Experiments with other mutants are consistent with this suggestion. The structure of the isosteric mutant T72V has been studied in detail (*9*, *10*). Its structure is identical to that of the wild type except for water molecules in the T state interface between the subunits. Its rates of combination with O_2 and CO are much faster, and there is a 40-fold increase

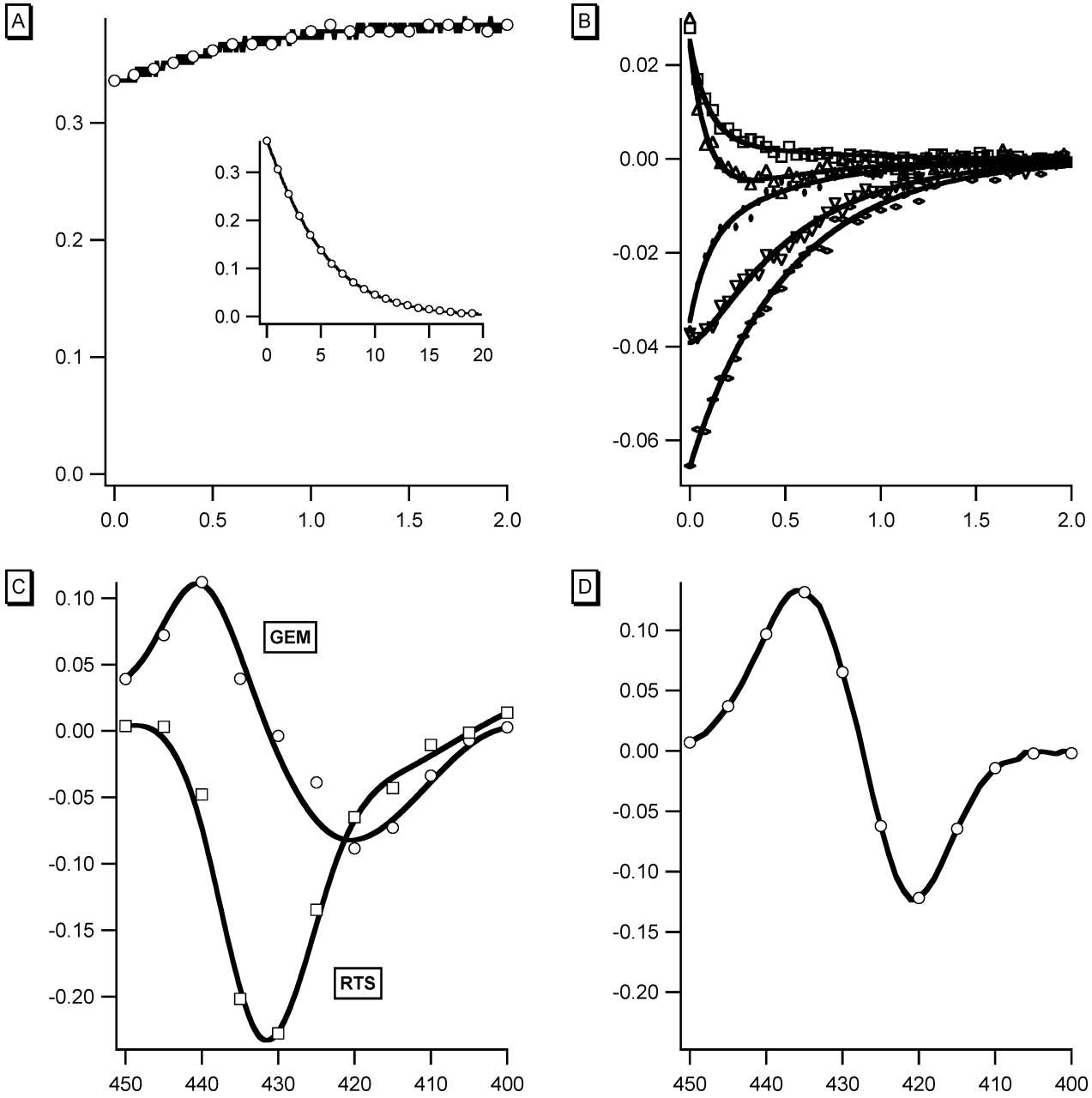

FIGURE 1: (A) Absorbance change at 435 nm during the first 2 μs (abscissa) after photolysis. At the beginning of the curve, the absorbance (ordinate) increases after the flash. The *rts* is the relatively slow change that follows. Conditions: 1 mM CO, 18 μM heme, 0.05 M KP_i, 20 °C, and path length of 2 mm. The inset shows the complete rebinding of CO, on an abscissa of 20 ms. (B) Data for five representative wavelengths from the same experiment, on an expanded scale. The abscissa is 2.0 μs. The ordinate is the change in absorbance. Points are experimental; the lines are fits to two exponentials using the same rates for all traces. Full photolysis was used in the experiment. (C) Coefficients for the rates used in panel B plotted vs wavelength. Rates were 1.9×10^7 s^{-1} for curve GEM (geminate) and 2.9×10^6 s^{-1} for curve RTS (*rts*). (D) Static difference spectrum of Hb_2 minus $Hb_2(CO)_2$ for comparison with curve GEM of panel C.

in the affinity for oxygen, coupled to an increase in Hill's *n* from 1.45 to 1.55. These findings may be accommodated in the MWC model by a decrease in the allosteric parameter *L* without a change in the intrinsic T and R properties (*9*). At equilibrium, the distribution of R and T is quite different from that of the wild type: $Hb_2(CO)_2$ and Hb_2CO are effectively all in the R state, and even Hb_2 is ~10% R. Within the first few microseconds of photolysis, in addition to a geminate reaction, there is an *rts* signal with the same spectrum as the slower broader wild-type *rts* signal. Unlike that of the wild type, however, its appearance is accurately described by the single rate constant of 1.0×10^5 s^{-1} at all levels of photolysis. With a value of 10 for *L* and the standard value of 600 for *c*, Hb_2CO is 98% R state and $Hb_2(CO)_2$ is almost all R state; thus, the change from $Hb_2(CO)_2$ to Hb_2CO would not be expected to contribute a significant *rts* change. The observed *rts* must therefore be attributed to the change from Hb_2CO to Hb_2, and it has the form of the broader spectrum of Figure 2, already attributed to this change in the wild type. When the flash intensity is changed, the amplitude of the *rts* signal scales with the square root of photolysis, consistent with a relation between the *rts* signal and the change of Hb_2CO from R to T.

The absence of an *rts* signal in all mutants at position 97 suggests that it may be linked to the effect of Phe 97 packing against the heme in the T state. Raman studies (*12*) with

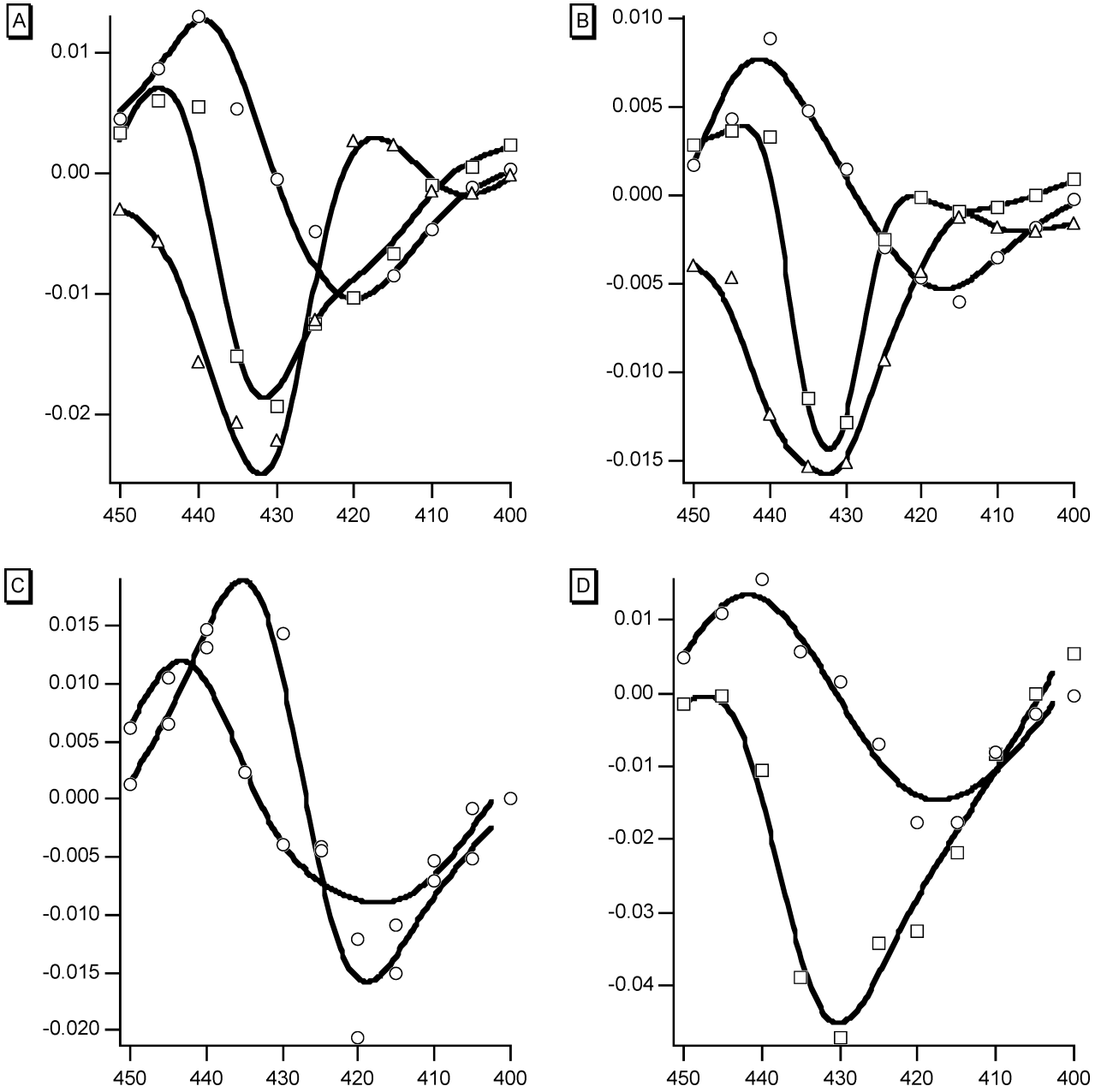

FIGURE 2: Weights of the components used to represent the absorbance changes (ordinates) during the first 2 μs after photolysis of the indicated mutants. In each panel, the curve with the highest point is assigned to geminate rebinding of ligand. In panels A (wild type) and B (L73M), the middle spectrum is assigned to the *rts* signal of Hb_2 and the bottom spectrum is assigned to $Hb_2(CO)$. (C) Two geminate recombination spectra associated with F97Y. (D) One and only *rts* spectrum associated with T72V. In all panels, the abscissa is wavelength in nanometers.

wild-type HbI have identified resonances that follow a time course following CO photodissociation approximately similar to that observed here for the *rts.* Among these changes, the heme macrocycle resonance at 756 cm^{-1} and the iron-proximal histidine stretching mode at 203 cm^{-1} may be correlated with the R to T transition of Phe 97 and thus may be related to the *rts* signal observed here. The *rts* time course is slightly faster than that suggested by time-resolved crystallography (*13*), which probably reflects real differences between crystalline and solution experiments.

Rate of the R−T Transition. Measurement of the rate of appearance of the *rts* signal immediately raises the question of its relation to the rate of change of the functional properties of the protein. One approach was to use the laser flash to generate empty sites suddenly and follow the bimolecular reaction thereafter. The first mutant that was examined was T72V reacting with 1 atm of CO. The time of observation was extended to include bimolecular recombination over a 4000-fold range of intensities. Two rates, 1.8 and 5.2 μM^{-1} s^{-1}, were attributed to binding to T and R states, respectively. In this experiment, the doubly liganded species should be more than 99.9% R state, so the immediate photoproduct is expected to be in the R state. The finding of a low rate of binding shows that T state function appears quickly, but quantitation is complicated by a small amount of protein with R state properties that does not appear to enter into allosteric reactions. The proportion of the main reaction ascribed to the slower (1.8 μM^{-1} s^{-1}) component (Figure 4) increases at high light levels as the proportion of Hb_2 relative to Hb_2-CO increases; it fails to reach 100% at high light intensity,

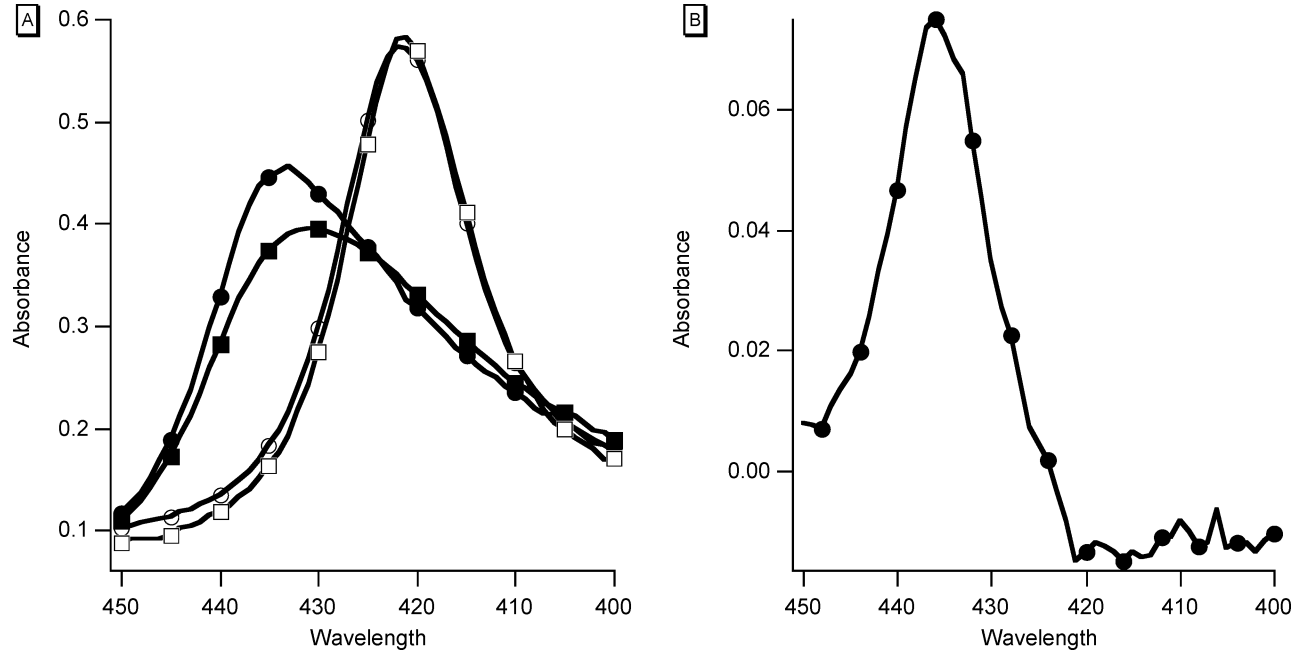

FIGURE 3: (A) Absorption spectra of the wild type [deoxy (●) and CO (○)] and F97Y [deoxy (■) and CO (□)]. (B) Difference spectrum of F97Y Hb_2 minus wild-type Hb_2. The heme concentration was 4 μM, and the path length was 1 cm.

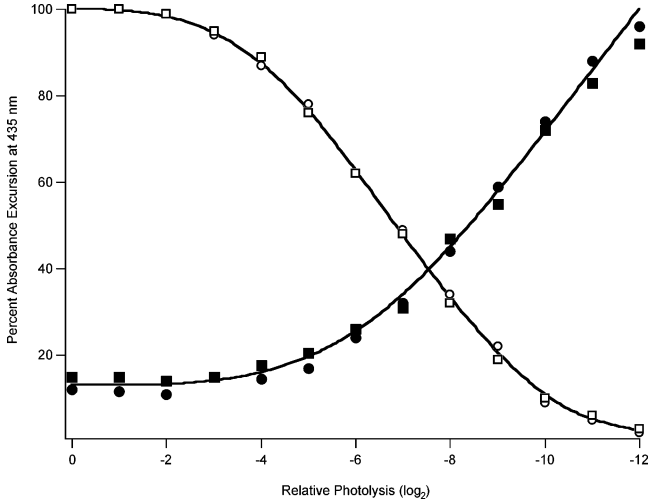

FIGURE 4: Binding of CO to T72V. The abscissa is $\log_2$ relative photolysis intensity. Absorbance excursion at 435 nm, percent of value with full light [(□) 1 mM CO and (○) 0.1 mM CO] and the corresponding fraction of the faster reaction [(■) 1 mM CO and (●) 0.1 mM CO]. The path length was 1 mm, with a 6 ns flash.

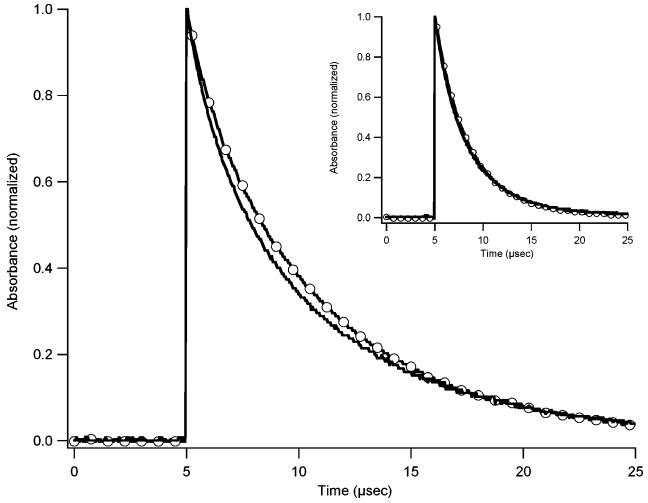

FIGURE 5: Binding of CO (0.1 mM) to T72V followed at 435 (−○−) and 420 nm (—). The inset shows results for sperm whale myoglobin treated similarly.

tending toward an asymptote at 88% of the total absorbance change. Repetition of the experiment with 10% CO in place of 1 atm of CO yielded similar results, eliminating ligand binding kinetics as a source of the anomaly. A further point of interest arises when CO binding is followed at several wavelengths. With the parameters given previously and with full photolysis, most of the hemoglobin is in the T state very soon after dissociation of CO. As binding proceeds, the R state accumulates and the *rts* signal is reversed. The result is that the measured course of ligand binding should not be quite the same at different wavelengths. The effect, though small, is quite demonstrable. The time course of binding of CO to T72V is slightly different when followed at 435 and at 425 nm (Figure 5). The data from a control experiment with myoglobin (inset) share the same time course at these wavelengths.

The rapid appearance of the *rts* signal in the wild type (2.0×10^6 s^{-1}) suggested it might well precede the functional change of R to T. With a large value of L (4.8×10^4), however, even if this rate were also the rate of appearance of T state ligand binding, the rate of the T_0-R_0 reaction ($2.0 \times 10^6 \times L$) would only be ~20 s^{-1}. A qualitative test of this rate was made by comparing the time courses of CO binding with 10% CO and with 1 atm of CO. An accelerating time course had been reported earlier in a flash photolysis experiment using 10% CO (*2*). If the T_0-R_0 rate is only 20 s^{-1}, the rate of binding with 1 atm of CO, some 150 s^{-1}, would be too great to allow significant acceleration to develop, with binding to the T state only. Experiments (Figure 6) confirmed the earlier result with 10% CO, whereas acceleration with 1 atm of CO was negligible. It appears that the T_0 to R_0 time course cannot be much greater than ~20 s^{-1} so that the appearance of the *rts* signal and the change from R to T must share the same rate. Additional

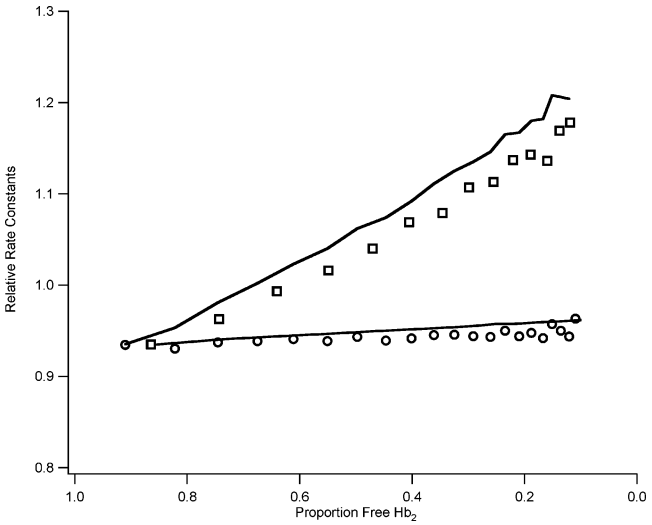

FIGURE 6: Combination of 1 mM CO (○) and 0.1 mM CO (□) with the wild type followed at 435 nm. The abscissa is the proportion of free Hb_2. The ordinate shows corresponding relative rate constants obtained by smoothing the 400 total data points using a moving average of five points. Rates were calculated from point to point. The lowest point (ordinate) corresponds to 0.18 μM^{-1} s^{-1} and the highest to 0.27 μM^{-1} s^{-1}.

steps may precede and follow the *rts* signal but must be rapid compared with the rate of the ligand reactions. The corollary is that the R_0 to T_0 rate of appearance of T state function should be the same as that of the appearance of the *rts* signal (2.0×10^6 s^{-1}).

The reaction of the wild type with oxygen is faster and more difficult to address; the effective quantum yield is low, pointing to picosecond or faster geminate reactions. Nanosecond geminate rebinding also returns 45% of photodissociated oxygen to the heme contributing to a mix of R and T states, presumably in a binomial distribution. The resulting initial rate of oxygen rebinding is therefore intermediate between R and T state rates and, in the practically accessible range, is very slightly dependent on the amplitude of photolysis. The initial rate observed with 1 atm of O_2 following photolysis of Hb_2O_2 was 17 μM^{-1} s^{-1}. To increase the proportion of Hb_2 after the laser flash, the sample was equilibrated with CO and O_2 gases in an 80:20 ratio. The value of *M* (the ratio of the affinities for O_2 and CO of the second molecule of the ligand to bind) is 200 (*1*), so effectively, all the protein is present as Hb_2CO and is largely in the R state. The full flash removes more than 99% of bound CO in 5 ns, delivering R state Hb_2. Relaxation after the flash was followed at six wavelengths in the Soret region. The results were modeled using the standard R state rates and T state values for oxygen (*7*) together with the revised value of *L* and a separate measurement of the T state combination rate for CO on the same sample. The T state rate of combination was the only variable that was used. The rms residual was 0.0016 and the oxygen on rate 17 μM^{-1} s^{-1}. There is no evidence of the R state rate of 40 μM^{-1} s^{-1}, corresponding to a pseudo-first-order rate of 60 000 s^{-1} with 1 atm of O_2. Although the experiment does not lead to a numerical value, the rate of the functional R to T change must be at least 1.0×10^5 s^{-1}, and no steps slower than that can be prerequisites of the functional R to T transition in the wild type. Note that the rate constant for binding of oxygen to the T state was significantly greater than previously suggested (*1*, *7*).

Application of the Model to Other Mutants. As suggested by Edelstein (*11*), the rough relation between the cooperativity of naturally occurring hemoglobin mutants and their affinity might be explained if T and R states were shared by several hemoglobins which would then have widely different values of *L*. His proposal could not be tested fully because of difficulty in determining the value of *L*, though a clear relation between affinity and Hill's *n* was found. By analogy, for *Scapharca*, if the affinity of the mutant F97Y sets a standard for a general R state, there should be no mutants with higher affinity, and indeed, none has yet been found. Similarly, if the T state of the wild type defines a standard T state, there should be no mutant with a dissociation constant for oxygen of >47 μM. The mutant L73M has a dissociation constant of 33 μM (cf. the wild-type value of 16 μM) and has been examined with the Edelstein proposal in mind.

The value of *L* for L73M has been estimated in two different ways. In kinetic experiments, assuming the standard parameters, with *L* as the sole variable, its value was 6.1×10^5. Computer runs with slightly different values for the kinetic parameters showed that the sensitivity of the solutions to the value of *L* was low because *L* is already so large. The equilibrium curve calculated from the same set of parameters and p_{50} gave an *L* of 5.5×10^5 but a lower *n* of 1.18 (observed value of 1.24). With these numbers, 55% of fully liganded Hb_2O_2 remains in the T state so the amplitude of the *rts* is reduced (Figure 2). When the appearance of the *rts* was represented by two exponentials, the apparent rate of the *rts* component fell off as the level of photolysis was reduced and its spectrum (Figure 7A) changed in shape. The data permitted analysis with three exponentials. The fastest rate had the form of a ligand binding difference spectrum. The spectrum associated with the lowest rate has the same form as the *rts* spectrum of T72V, already identified with the change of Hb_2 from R to T. The contributions of the two *rts* components are strongly dependent on level of photolysis (Figure 7B). The lines in the figure show the change in the amounts of Hb_2 and Hb_2CO appearing on photolysis calculated from the model. Although the scatter of the points is large reflecting the small absorbance changes, there is little doubt that the data form two groups. The identification of the R to T changes of Hb_2 and Hb_2CO with the faster and slower *rts* signals is also clear. The top curve in Figure 7B refers to the fast component and the bottom curve to the slower component.

With a value of *L* that is so large, singly liganded hemoglobin should be more than 99% T state, which would predict no observable difference in rates for different levels of photolysis. This was examined in experiments with CO. There was no clear difference between the rates of rebinding following full and partial photolysis with both giving a rate of 0.1 μM^{-1} s^{-1}. The rate of binding of oxygen to T state L73M was measured by equilibrating a sample with 80% CO and 20% O_2. The rate for T state binding was 11.5 μM^{-1} s^{-1}, regarded as being the same as the rate for the wild type (Table 1). This is the result expected on the Edelstein principle.

Results with the mutant F97L are particularly interesting both because it was the first mutant prepared (*7*) and because

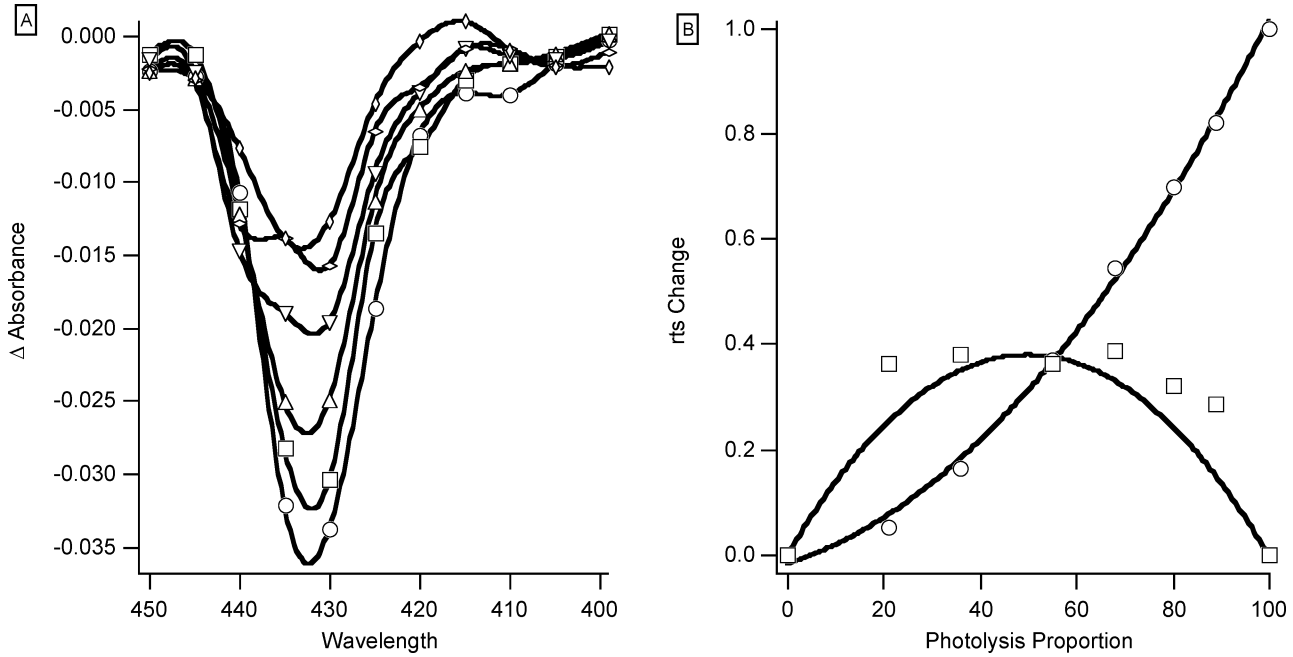

FIGURE 7: (A) Spectra of *rts* components for L73M. The ordinate is the absorbance change for six photolysis intensities. The photolysis intensity was halved between each record. The abscissa is the wavelength in nanometers. (B) L73M *rts* coefficients and photolysis. The ordinate shows (○) the faster *rts* signal associated with Hb_2 R to T change and (□) the slower *rts* signal associated with $Hb_2(CO)$. Lines represent simulations of each signal; symbols are experimental data. The abscissa is the proportion of photolysis.

Table 1: Parameters Describing Binding of Oxygen to Some Mutants[a]

						$[O_2]_{50}$		*n*	
	L	T_{on}	T_{off}	rms	$CO_{T_{on}}$	calcd	obsd	calcd	obsd
wild type	48000	10	500	0.0027	0.2	16.6	16.2	1.54	1.47
T72V	5	0	550	0.0051	0.2	0.2	0.3	1.43	1.55
L73M	650000	11.6	550	0.0014	0.15	31.9	34.3	1.24	1.24
F97L	330	33	47	0.0025	0.5	1.0	1.6	1.16	1.15
I114F	210000	4.8	200	0.0015	0.2	26.5	34	1.22	1.08

[a] *L* is the Hb_T/Hb_R ratio for deoxyhemoglobin. T_{on} is the rate of combination of oxygen with T state hemoglobin, in units of micromolar per dimer per second. T_{off} units are inverse seconds. rms is the square root of the sum of the squares of differences between observed and calculated values of absorbance for all points in an experiment (usually 14 000). $CO_{T_{on}}$ units as for oxygen. $[O_2]_{50}$ is the concentration of oxygen (micromolar) required to give half-saturation using the kinetic parameters listed in the allosteric model. *n* is Hill's *n*, a measure of sigmoidicity. For a dimer, its limits are 1 (no cooperativity) and 2 (full cooperativity). Note that due to experimental error, the results of individual experiments given in the text may not agree with the averaged values listed here.

of its behavior. The substitution did not lead to a total loss of cooperativity with Hill's *n* decreasing from 1.45 to 1.16 coupled with a 8-fold increase in affinity. The spectra in the usual time frame, however, show no sign of an *rts* signal, but there are two difference spectra. The faster (2.7×10^7 s^{-1}) has an isosbestic point at 433 nm in a ligand binding difference spectrum; the slower rate (3.9×10^6 s^{-1}) also has a ligand binding spectrum with an isosbestic point at 425 nm. In this respect, F97L resembles F97Y. The standard 35-trace data set was treated as described for the wild type and L73M varying *L* only. The results were unacceptable. The rms residual was 0.0057 with an *L* of 1280. Hill's *n* was 1.8, very far from the experimental value of 1.16, though p_{O_2} at 1.6 mmHg was not far from the experimental value. This mutant, though demonstrating the importance of residue F97, is not represented satisfactorily by the two-state model with the constraints of "standard" R and T states. The failure of this analysis is reasonable, however, given that crystal structures indicate that the R and T states of F97L are likely to be quite different from those of the wild type (*7*).

Another mutant, I114F, has low affinity and reduced cooperativity ($p_{50} = 21$ mmHg; $n = 1.08$), although it has an *rts* signal similar to that of the wild type. The results of the 35-trace experiment, constrained by standard R and T states, gave quite different values, and as with F97L, new values had to be sought. It was found that the on rates for both R and T states had to be reduced substantially to the values given in Table 1. Modification of the standard values may make suggestions about mechanism; in this case, as both R and T on rates must be substantially reduced, the Phe at position 114 may be blocking a pathway for ligands.

CONCLUSIONS

The origin of the *rts* is not known; it has not been observed in any mutant at position 97 and to that extent is linked to that residue. Although not quite as fast, *rts* occurs in the same time range as geminate recombination, and examination of the transient spectra is required to establish the nature of the absorbance changes during the first 2 μs after photolysis. The experiments and calculations described in the main section of this paper may be summarized by saying that the two-state model affords an internally consistent description of ligand binding kinetics by all of the mutants so far examined except for F97L and I114F. This does not, of course, prove that is how the protein reacts. The model may be used to classify mutants into those whose behavior may be described by change in allostery and those where access to the heme group or change in its intrinsic reactivity is more significant. It may, indeed, be necessary to use the model to describe kinetic data generally because the phenomenological rates are all, to a greater or lesser extent, composites of several allosteric and kinetic parameters. The rate of com-

bination of oxygen, for example, may be influenced by the extent of geminate combination, the length of a photolysis flash, the rate of the R_0 to T_0 transition, and the partition of Hb_2O_2 between R and T states, as well as by the on and off rates for ligands. The precision of the allosteric parameters is not readily accessible; experience suggests between 5 and 10% may prove reasonable except for *L* which, as its influence is indirect, may have an uncertainty of ≥30%.

The rate of dissociation of oxygen from the wild type is given by the proportion of T multiplied by the rate of dissociation plus the proportion of R multiplied by the rate of dissociation. This is $0.15 \times 500 + 0.85 \times 3 = 78\ s^{-1}$, a rate in reasonable agreement with experiment ($100\ s^{-1}$). Analogous calculations for L73M lead to rates of several hundreds per second. The observed rate with dithionite is high but poorly determined because the time required by dithionite to react with oxygen in physical solution is on the same order as that of oxygen dissociation. The dissociation reaction is certainly rapid, however. The work described here with *Scapharca* appears to have fulfilled the expectation and hopes raised for a dimeric hemoglobin in the introductory section. The two-state model has often been used in describing ligand binding experiments and with carbon monoxide, sometimes with very great precision (*14*). We believe that this may be the first time a complete description of binding of oxygen to a cooperative hemoglobin has been given in terms of the allosteric model in which values of the allosteric parameters were supported by both kinetic and equilibrium experimental data.

REFERENCES

1. Chiancone, E., Elber, R., Royer, W. E., Regan, R., and Gibson, Q. H. (1993) Ligand binding and conformation change in the dimeric hemoglobin of the clam *Scapharca inaequivalvis*, *J. Biol. Chem. 268*, 5711−5718.
2. Antonini, E., Ascoli, F., Brunori, M., Chiancone, E., Verzili, D., and Gibson, Q. H. (1984) Kinetics of ligand binding and quaternary conformational change in the homodimeric hemoglobin from *Scapharca inaequivalvis*, *J. Biol. Chem. 259*, 6730−6738.
3. Monod, J., Wyman, J., and Changeux, J. P. (1965) On the nature of allosteric transitions: A plausible model, *J. Mol. Biol. 12*, 86−118.
4. Condon, P. J., and Royer, W. E. (1994) Crystal structure of oxygenated *Scapharca* dimeric hemoglobin at 1.7-Å resolution, *J. Biol. Chem. 269*, 25259−25267.
5. Royer, W. E. (1994) High-resolution crystallographic analysis of a co-operative dimeric hemoglobin, *J. Mol. Biol. 235*, 657−681.
6. Mozzarelli, A., Bettati, S., Rivetti, C., Rossi, G. L., Colotti, G., and Chiancone, E. (1996) Cooperative Oxygen Binding to *Scapharca inaequivalvis* Hemoglobin in the Crystal, *J. Biol. Chem. 271*, 3627−3632.
7. Pardanani, A., Gibson, Q. H., Colotti, G., and Royer, W. E. (1997) Mutation of residue Phe97 to Leu disrupts the central allosteric pathway in *Scapharca* dimeric hemoglobin, *J. Biol. Chem. 272*, 13171−13179.
8. Knapp, J. E., Nichols, J. C., Gibson, Q. H., and Royer, W. E., Jr. (2005) Central role of residue F4 in modulating oxygen affinity and cooperativity in *Scapharca* dimeric hemoglobin, *Biochemistry 44*, 14419−14430.
9. Royer, W. E., Jr., Pardanani, A., Gibson, Q. H., Peterson, E. S., and Friedman, J. M. (1996) Ordered water molecules as key allosteric mediators in a cooperative dimeric hemoglobin, *Proc. Natl. Acad. Sci. U.S.A. 93*, 14526−14531.
10. Pardanani, A., Gambacurta, A., Ascoli, F., and Royer, W. E. (1998) Mutational destabilization of the critical interface water cluster in *Scapharca* dimeric hemoglobin: Structural basis for altered allosteric activity, *J. Mol. Biol. 284*, 729−739.
11. Edelstein, S. J. (1971) Extensions of the allosteric model for haemoglobin, *Nature 230*, 224−227.
12. Rousseau, D. L., Song, S., Friedman, J. M., Boffi, A., and Chiancone, E. (1993) Heme-Heme Interactions in a Homodimeric Cooperative Hemoglobin: Evidence from Transient Raman Scattering, *J. Biol. Chem. 268*, 5719−5723.
13. Knapp, J. E., Reinhard, P., Srajer, V., and Royer, W. E., Jr. (2006) Allosteric action in real time: Time-resolved crystallographic studies of a cooperative dimeric hemoglobin, *Proc. Natl. Acad. Sci. U.S.A. 103*, 7649−7654.
14. Henry, E. R., Jones, C. M., Hofrichter, J., and Eaton, W. A. (1997) Can a Two-State MWC Allosteric Model Explain Hemoglobin Kinetics? *Biochemistry 36*, 6511−6528.

BI061451K